INTERNATIONAL JOURNAL FOR NUMERICAL METHODS IN ENGINEERING
Int. J. Numer. Meth. Engng 2006; **00**:1–15 *Prepared using* nmeauth.cls *[Version: 2002/09/18 v2.02]*

Crack tip enrichment in the XFEM method using a cut-off function

Elie Chahine[1,*] Patrick Laborde[2], Yves Renard[3]

[1] *Institut de Mathématiques, UMR CNRS 5215, GMM INSA Toulouse, Complexe scientifique de Rangueil, 31077 Toulouse Cedex 4, France, elie.chahine@insa-toulouse.fr*
[2] *Institut de Mathématiques, UMR CNRS 5215, UPS Toulouse 3, 118 route de Narbonne, 31062 Toulouse cedex 4, France, patrick.laborde@math.ups-tlse.fr*
[3] *Institut Camille Jordan, CNRS UMR 5208, INSA de Lyon, Université de Lyon, 20 rue Albert Einstein, 69621 Villeurbanne Cedex, France, yves.renard@insa-lyon.fr*

SUMMARY

We consider a variant of the eXtended Finite Element Method (XFEM) in which a cut-off function is used to localize the singular enrichment surface. The goal of this variant is to obtain numerically an optimal convergence rate while reducing the computational cost of the classical XFEM with a fixed enrichment area. We give a mathematical result of quasi-optimal error estimate. One of the key points of the paper is to prove the optimality of the coupling between the singular and the discontinuous enrichments. Finally, we present some numerical computations validating the theoretical result. These computations are compared to those of the classical XFEM and a non-enriched method. Copyright © 2006 John Wiley & Sons, Ltd.

KEY WORDS: fracture mechanics; extended finite element method; cut-off function; error estimates; Numerical convergence rate.

1. Introduction

The benefits of computational methods using classical finite element strategies are limited when solving problems defined over cracked domains and that for at least two reasons: the mesh should be sufficiently refined around the crack tip to model the singular strain, and the domain should be remeshed step by step according to the geometry of the crack propagation. To overcome these difficulties and to make the finite element methods more flexible, many approaches have been studied. In 1973, Strang and Fix [1] introduced a singular enrichment method using a cut-off function for a mesh dependent on the domain geometry. Since then, different approaches had been analyzed such the PUFEM (the Partition of Unity Finite Element Method, see [2]), the Arlequin method (see [3]), the GFEM (Generalized Finite Element Method, see [4, 5]), the XFEM (eXtended Finite Element Method) and the patches

*Correspondence to: Institut de Mathématiques, UMR CNRS 5215, GMM INSA Toulouse, Complexe scientifique de Rangueil, 31077 Toulouse, France, elie.chahine@insa-toulouse.fr

Received 5 December 2006
Revised

enrichment approach (see [22]).

Inspired by the PUFEM, the XFEM was introduced by Moës and *al.* in 1999 (see [6, 7]). The idea of XFEM consists in enriching the basis of the classical finite element method by a step function along the crack line to take into consideration the discontinuity of the displacement field across the crack and by some non-smooth functions representing the asymptotic displacement around the crack tip. The latter enrichment is the so-called singular enrichment. This enrichment strategy allows the use of a mesh independent of the crack geometry. Since the introduction of the XFEM, many works have been achieved in order to explore the capabilities of the XFEM and improve its accuracy as in [15, 16, 17, 18, 19, 20, 21]. Other works studied XFEM with some 3D applications as [8, 9, 10, 11, 12, 13, 14].

In spite of the singular enrichment of the finite element basis, the obtained convergence error of XFEM remains only in $\sqrt{h}$ if linear finite elements are used (see [23], h being the mesh parameter). To improve this result and obtain an optimal accuracy, many developments have been performed. A first idea was to enrich the degrees of freedom of a whole area around the crack tip by the singular functions (see [23, 24]). In a second variant, a global enrichment strategy is considered in order to reduce the number of the enrichment degrees of freedom and improve the conditioning of the linear system. Such a variant is a non-conforming method to deal with the difficulty of transition between the enriched area and the remaining elements of the mesh [23].

We consider in this paper another variant of XFEM which allows to benefit from the advantages of the latter one while preserving the conformity of the method. One of the difficulties is the mathematical analysis of the coupling between the two types of enrichment. The detailed proof of the optimal convergence results, that were announced in [25], is studied in the present paper. Moreover, these results are validated by some numerical computations and comparisons with a non-enriched method and the classical XFEM. These numerical results show that the proposed variant preserves an optimal convergence even though its computational cost is lower than that of XFEM.

The elastostatic problem is presented in Section 2 for a two-dimensional cracked domain. In Section 3, we introduce the proposed variant in which the linear finite element basis is enriched with singular functions using a cut-off function. In Section 4, a mathematical result is given showing the accuracy of the method. To prove the error estimate, the domain Ω is splitted into two subdomains and an interpolation operator is defined using an extension operator over each subdomain. Then we obtain a quasi-optimal rate of convergence by means of this interpolation operator considered on every type of triangles: triangle containing the crack tip and triangles partially or totally enriched with the discontinuous function. In Section 5, some numerical results are presented including a comparison with a non-enriched method and the XFEM using a singular enrichment over a whole area. These results show an optimal rate of convergence and a satisfactory conditioning.

2. The model problem

Let Ω be a bounded cracked domain in $\mathbf{R}^2$; the crack Γ_C is assumed to be straight. We consider the linear elasticity problem on this domain for an isotropic material. The boundary of Ω, denoted $\partial\Omega$, is partitioned into Γ_D where a Dirichlet condition is prescribed, Γ_N with a Neumann condition and Γ_C (the crack) where a traction free condition is considered (Fig. 1).

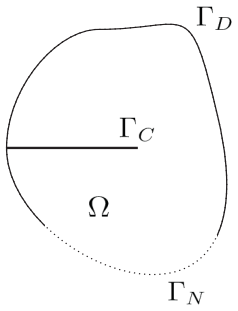

Figure 1. *The cracked domain* Ω.

Let $\vartheta = \{v \in H^1(\Omega);\ v = 0 \text{ on } \Gamma_D\}$ be the space of admissible displacements and

$$\begin{aligned} a(u,v) &= \int_\Omega \sigma(u) : \varepsilon(v)\ dx, \\ l(v) &= \int_\Omega f.v dx + \int_{\Gamma_N} g.v\ d\Gamma, \\ \sigma(u) &= \lambda tr\varepsilon(u) I + 2\mu\varepsilon(u), \end{aligned} \tag{1}$$

where $\sigma(u)$ denotes the stress tensor, $\varepsilon(u)$ the linearized strain tensor, f and g are some given force densities on Ω and Γ_N respectively, and $\lambda > 0$, $\mu > 0$ are the Lamé coefficients. To simplify the mathematical analysis, we consider a homogeneous Dirichlet boundary condition on Γ_D. The extension to a non-homogeneous condition is straightforward. The problem can be written

$$\text{Find} \quad u \in \vartheta \quad \text{such that} \quad a(u,v) = l(v) \quad \forall v \in \vartheta. \tag{2}$$

We suppose that f and g are smooth enough to let the solution u of the elasticity problem be written as a sum of a singular part u_s and a regular part $u - u_s$ in Ω (see [26, 27]) satisfying for a fixed $\epsilon > 0$ (see [30] for the definition of $H^s(\Omega),\ s \in \mathbf{R}$):

$$u - u_s = u - (K_I u_I + K_{II} u_{II}) \in H^{2+\epsilon}(\Omega), \tag{3}$$

where K_I and K_{II} denote the stress intensity factors. The asymptotic displacement at the crack tip is defined from functions u_I and u_{II}, respectively the opening mode and the sliding

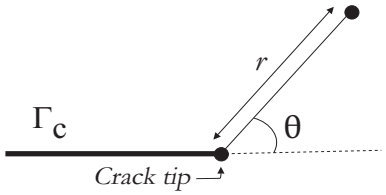

Figure 2. *Polar coordinates respectively to the crack tip* Ω.

mode for a two-dimensional crack given in polar coordinates by (see [28, 29]):

$$u_I(r,\theta) = \frac{1}{E}\sqrt{\frac{r}{2\pi}}(1+\nu)\begin{pmatrix} \cos\frac{\theta}{2}(\delta-\cos\theta) \\ \sin\frac{\theta}{2}(\delta-\cos\theta) \end{pmatrix}, \tag{4}$$

$$u_{II}(r,\theta) = \frac{1}{E}\sqrt{\frac{r}{2\pi}}(1+\nu)\begin{pmatrix} \sin\frac{\theta}{2}(\delta+2+\cos\theta) \\ \cos\frac{\theta}{2}(\delta-2+\cos\theta) \end{pmatrix}, \tag{5}$$

where ν denotes the Poisson ratio, E the Young modulus, $\delta = 3-4\nu$ in the plane stress problem and (r,θ) the polar coordinates respectively to the crack tip (fig. 2). The normal (respectively tangential) component of function u_I(respectively u_{II}) is discontinuous along the crack. Note that u_I and u_{II} belong to $H^{3/2-\eta}(\Omega)$ for any $\eta > 0$ (see [26]) which limits the order of the convergence rate of the classical finite element method to $h^{1/2}$.

3. Discrete problem

The idea of the classical XFEM (see [6, 7]) is to use a finite element space enriched with some additional functions. The finite element method is defined independently from the crack on a mesh of the non-cracked domain $\overline{\Omega}$. At the nodes whose corresponding shape function support is cut by the crack, an enrichment function of Heaviside type is considered:

$$H(x) = \begin{cases} +1 & \text{if } (x-x^*)\cdot\ n\ \geq\ 0, \\ -1 & \text{elsewhere,} \end{cases} \tag{6}$$

where x^* denotes the crack tip and n is a given normal to the crack. Moreover, the nodes of the triangle containing the crack tip are enriched with the following singular functions given in polar coordinates:

$$\{F_j(x)\}_{1\leq j\leq 4} = \{\ \sqrt{r}\sin\frac{\theta}{2}, \sqrt{r}\cos\frac{\theta}{2}, \sqrt{r}\sin\frac{\theta}{2}\sin\theta, \sqrt{r}\cos\frac{\theta}{2}\sin\theta\ \}, \tag{7}$$

(fig.3). We recall that

$$F_j \in H^{3/2-\eta}(\Omega),\ \forall\eta>0, j=1,..,4. \tag{8}$$

In the following, we use the fact that

$$F_j \in C^2(\Omega\setminus\{x^*\}). \tag{9}$$

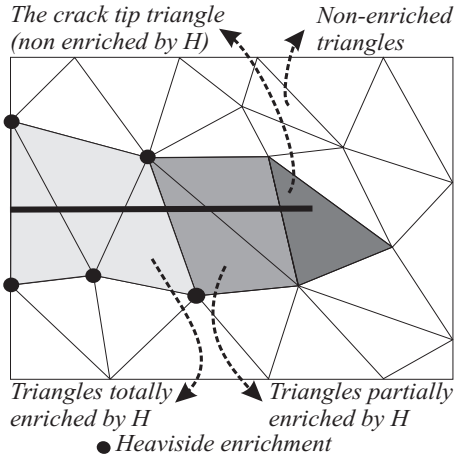

Figure 3. *Enrichment strategy.*

Since the mesh is independent of the crack geometry, the Heaviside function represents the discontinuity of the displacement field along the crack and the singular functions allow to take into account the asymptotic displacement at the crack tip. Such a method enables to discretize the domain without explicitly meshing the crack surfaces, and hence the crack propagation simulations can be done without remeshing.

For the model problem, we consider a Lagrange finite element method of first order defined on a regular triangulation of the non-cracked domain $\overline{\Omega}$. The piecewise P_1 basis functions are denoted φ_i (P_1 is the set of first degree polynomials). In the proposed variant of XFEM, we intend to enrich a whole area around the crack tip by using a cut-off function denoted χ. The XFEM enriched space of this variant is then

$$\vartheta^h = \left\{ v^h = \sum_{i\in I} a_i\varphi_i + \sum_{i\in I_H} b_i H\varphi_i + \sum_{j=1}^{4} c_j F_j\chi;\ a_i, b_i, c_j \in \mathbf{R}^2 \right\}, \tag{10}$$

where

- h is the mesh parameter and $\mathcal{T}_h$ is a regular triangulation (in the sense of the Ciarlet [31]) of the non-cracked domain $\overline{\Omega}$,
- I is the set of node indices of the classical finite element method,
- I_H is the set of node indices enriched by the Heaviside function given by (6)
- $F_j,\ j = 1, .., 4$, are the singular functions given by (7)
- χ is a C^2 cut-off function such that there exists $0 < r_0 < r_1$ with

$$\begin{cases} \chi(r) = 1 \text{ if } r < r_0, \\ 0 < \chi(r) < 1 \text{ if } r_0 < r < r_1, \\ \chi(r) = 0 \text{ if } r_1 < r. \end{cases} \tag{11}$$

The discrete problem can be written as follows

$$\text{Find} \quad u^h \in \vartheta^h \quad \text{such that} \quad a(u^h, v^h) = l(v^h) \quad \forall v^h \in \vartheta^h. \tag{12}$$

The proposed enrichment can be compared to the one of the classical XFEM, where the singular enrichment term of (10) is replaced by $\sum_{i\in I_s}\sum_{j=1}^{4} c_{ij}F_j\varphi_i$ and where I_s denotes the set of degrees of freedom of the element containing the crack tip. It can be compared also to the XFEM with pointwise matching (introduced in [23]). In the latter one, the singular enrichment term is written $\sum_{j=1}^{4} c_j F_j \Lambda$, where Λ is equal to one on the enriched area, and zero otherwise. On the node of the interface between the enriched zone and the rest of the mesh, a bonding condition is considered on the displacement field.

4. Error estimate

The mathematical result obtained in this work is the following:

Theorem 4.1. *Assume that the displacement field u, solution to Problem (2), satisfies Condition (3). Then, for any $\epsilon > 0$, the following estimate holds*

$$\|u - u^h\|_{1,\Omega} \leq Ch\|u - \chi u_s\|_{2+\epsilon,\Omega}, \tag{13}$$

where u^h is the solution to Problem (12), $\|.\|_{s,\Omega}$, $s \in \mathbf{R}$ stands for the norm in $H^s(\Omega)$ (see [30] for the definition of $\|.\|_{s,\Omega}$), u_s is the singular part of u (see (3)), χ is the C^2 cut-off function and finally $C > 0$ is a constant independent of h.

Remark. When using a classical finite element method over a cracked domain, the error is of order $\sqrt{h}$ while the displacement field belongs to $H^{3/2-\eta}$, $\forall\eta \geq 0$. The convergence rate obtained here is identical to the one obtained when using a classical finite element method of first order with a regular problem. The error estimate is not completely optimal due to the requirement $u - \chi u_s \in H^{2+\varepsilon}(\Omega)$ instead of $u - \chi u_s \in H^2(\Omega)$. This is strictly a technical difficulty.

In order to compute the interpolation error, we introduce an interpolation operator Π^h adapted to the problem. This is done by using an extension of the displacement field across the crack over $\overline{\Omega}$, then defining the interpolation of the displacement field using the extension (Lemma 4.3). The interpolation error estimates are then computed locally over every different type of triangles: triangles totally enriched by the discontinuous function (Lemma 4.4), triangles totally enriched by the singular functions (Lemma 4.5), triangles partially enriched by the discontinuous function (Lemma 4.6) and finally non-enriched triangles.

As mentioned above, the proof of Theorem 4.1 requires the definition of an interpolation operator adapted to the proposed method. Since the displacement field is discontinuous across the crack over Ω, we divide Ω into Ω_1 and Ω_2 according to the crack and a straight extension of the crack (fig.4). Let us denote $u_r = u - \chi u_s$, and u_r^k the restriction of u_r to Ω_k, $k \in \{1, 2\}$. As a result of (3), we can write that $u_r \in H^{2+\epsilon}(\Omega)$. There exists in $H^{2+\epsilon}$ an extension $\widetilde{u}_r^k$ of u_r^k across the crack over $\overline{\Omega}$ such that (see [30])

$$\|\widetilde{u}_r^1\|_{2+\epsilon,\overline{\Omega}} \leq C_1\|u_r^1\|_{2+\epsilon,\Omega_1}, \tag{14}$$

$$\|\widetilde{u}_r^2\|_{2+\epsilon,\overline{\Omega}} \leq C_2\|u_r^2\|_{2+\epsilon,\Omega_2}. \tag{15}$$

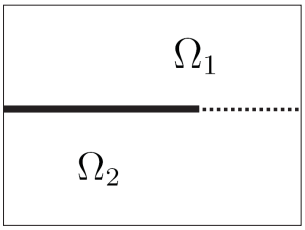

Figure 4. *Domain decomposition.*

The use of such extensions allows us to interpolate over complete triangles and not over sub-triangles or quadrangles that are inducted because of the presence of a crack.

In the following, C denotes a generic constant that might be different at each occurrence but is independent of h.

Definition 4.2. *Given a displacement field u satisfying (3) and two extensions $\widetilde{u}_r^1$ and $\widetilde{u}_r^2$ respectively of u^1 and u^2 in $H^{2+\epsilon}(\Omega)$, we define $\Pi^h u$ as the element of ϑ^h such that*

$$\Pi^h u \;=\; \sum_{i\in I} a_i\varphi_i \;+\; \sum_{i\in I_H} b_i H\varphi_i \;+\; \sum_{i=1}^{4} c_i F_i\chi, \tag{16}$$

where a_i, b_i are given as follows (x_i denotes the node associated to φ_i):

$$\begin{array}{l} \text{if } i \in \{I \setminus I_H\} \text{ then } a_i = u_r(x_i), \\ \text{if } i \in I_H \text{ and } x_i \in \Omega_k \text{ then } (k \in \{1,2\},\ l \neq k) \end{array} \left\{ \begin{array}{l} a_i = \frac{1}{2}\left(u_r^k(x_i) + \widetilde{u}_r^l(x_i)\right), \\ b_i = \frac{1}{2}\left(u_r^k(x_i) - \widetilde{u}_r^l(x_i)\right) H(x_i), \end{array} \right. \tag{17}$$

and c_i, $i = 1,..,4$ are derived from (4) and (5) such that $\sum_i c_i F_i = u_s$.

Lemma 4.3. *The function $\Pi^h u$ (Definition 4.2) verifies*
(i) $\Pi^h u = I^h u_r + \chi u_s$ over a triangle non-enriched by H,
(ii) $\Pi^h u|_{K\cap\Omega_k} = I^h \widetilde{u}_r^k + \chi u_s$ over a triangle K totally enriched by H,
where I^h denotes the classical interpolation operator for the associated finite element method.

Remark. Obviously, the definition of $\Pi^h u$ depends on the chosen extension $\widetilde{u}_r^k$. From Lemma 4.3, the function $\Pi^h u$ is called the XFEM interpolation of u. Note that (16) and equations *(i)* and *(ii)* of Lemma 4.3 define a unique XFEM interpolation function $\Pi^h u$ over the whole domain Ω. A similar construction of an interpolation operator taking only into account the discontinuity across the crack was done in [32]. The definition of $\Pi^h u$ that we introduce is adapted to the presence of singularities.

Proof. Equation *(i)* is directly derived from the first equation of (17) since I^h is the classical interpolation operator (see [31]). It means that a classical degree of freedom is equal to the node value of u_r if it is not enriched by H.

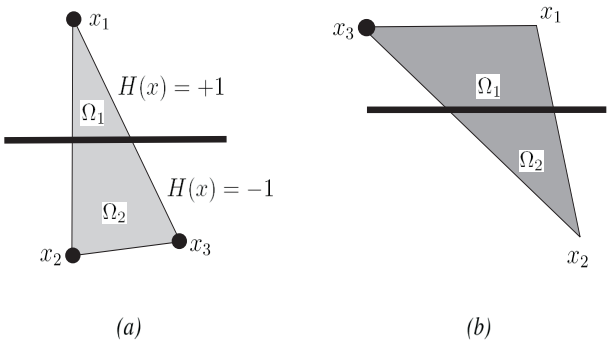

Figure 5. *(a) Totally enriched triangle and (b) partially enriched triangle (fig.3).*

In order to prove *(ii)*, we consider a triangle K totally enriched by the discontinuous function. Using local indexing, let the first node x_1 of K be in Ω_1 and the two others x_2 and x_3 be in Ω_2 (fig.5 (a)). Using (16), we have

$$\Pi^h u|_K = \sum_{j=1}^{3} a_j \varphi_j \ + \ \sum_{i=1}^{3} b_j H \varphi_j \ + \ \chi u_s, \tag{18}$$

where j denotes the local index of the degrees of freedom. Let p_k be the two polynomials defined by ($k \in \{1, 2\}$):

$$p_k = \Pi^h u|_{K \cap \Omega_k} - \chi us. \tag{19}$$

thus, we have

$$\begin{cases} p_1 = \displaystyle\sum_{j=1}^{3} a_j \varphi_j \ + \ \sum_{j=1}^{3} b_j \varphi_j, \\ p_2 = \displaystyle\sum_{j=1}^{3} a_j \varphi_j \ - \ \sum_{j=1}^{3} b_j \varphi_j. \end{cases} \tag{20}$$

Then, combining (20) and (17), we obtain

$$\begin{cases} p_1(x_j) = a_j + b_j = \widetilde{u}_r^1(x_j), \\ p_2(x_j) = a_j - b_j = \widetilde{u}_r^2(x_j). \end{cases} \tag{21}$$

We conclude that p_k is the classical interpolation of $\widetilde{u}_r^k$ over K, which gives *(ii)*. □

In order to find the global interpolation error, we will proceed by computing local error estimates over the triangles totally enriched by H, triangle containing the crack tip, triangles partially enriched by H and non-enriched triangles (fig.3). In what follows, let

$$h_L = \text{diam}(L) = \max_{x_1, x_2 \in L} |x_1 - x_2|, \tag{22}$$

and

$$\rho_L = \{\sup(\text{diam}(B));\ B \text{ ball of } \mathbf{R}^2,\ B \subset L\}, \tag{23}$$

where L is a subset of Ω.

Lemma 4.4. *Let $\mathcal{T}_h^H$ be the set of triangles totally enriched by H (fig.3) and $\sigma_K = h_K\rho_K^{-1}$. For all K in $\mathcal{T}_h^H$, and for all u satisfying (3) we have the estimates*

$$\|u - \Pi^h u\|_{1,K\cap\Omega_1} \leq Ch_K\sigma_K\|\widetilde{u}_r^1\|_{2,K}, \tag{24}$$

and

$$\|u - \Pi^h u\|_{1,K\cap\Omega_2} \leq Ch_K\sigma_K\|\widetilde{u}_r^2\|_{2,K}. \tag{25}$$

In fact, the triangles totally enriched by H are cut into two parts. Using the extensions of u_r^1 and u_r^2, we associate three interpolation points to every part. Thus the interpolation operator we defined, allows us to make a classical interpolation on every part of the triangle, and have the same optimal rate of convergence obtained in the classical global interpolation theorem (see [1, 33]). Thus, Lemma 4.4 is a direct consequence of this theorem.

Lemma 4.5. *Let K be the triangle containing the crack tip and $K^* = K\setminus\Gamma_C$. Using the same notations, we have the following estimate over K^**

$$\|u - \Pi^h u\|_{1,K^*} \ \leq \ Ch_K\sigma_K\|u - \chi u_s\|_{2+\epsilon,\Omega}, \tag{26}$$

where $\sigma_K = h_K\rho_K^{-1}$.

Proof. Since we added singular functions to the discrete space (around the crack tip), the singular part of u (see (3)) will be eliminated when we try to estimate $\|u - \Pi^h u\|_{1,K^*}$. Thus it is sufficient to estimate $\|u_r - \Pi^h u_r\|_{1,K^*}$ where $u_r = u - \chi u_s$. In fact

$$\|u_r - \Pi^h u_r\|_{1,K^*}^2 \ = \ \|u_r - \Pi^h u_r\|_{0,K^*}^2 \ + \ |u_r - \Pi^h u_r|_{1,K^*}^2, \tag{27}$$

where $|\cdot|$ denotes the H^1 semi-norm. Using Sobolev imbedding theorems (see [30]), the space $H^{2+\epsilon}(\Omega)$ (and not $H^2(\Omega)$) is continuously imbedded in $\mathcal{C}_B^1(\Omega)$, where $\mathcal{C}_B^1(\Omega) = \{v \in C^1(\Omega)$ such that $\nabla v \ \in L^\infty(\Omega)\}$ (see [30]). Thus

$$\|\nabla u_r\|_{L^\infty(\Omega)} \leq C\|u_r\|_{2+\epsilon,\Omega} = C\alpha \tag{28}$$

where

$$\|\nabla\Pi^h u_r\|_{L^\infty(K^*)} \leq \frac{C\alpha d}{\rho_K}, \tag{29}$$

where $d \leq h$ denotes the maximal distance between a node of K^* and the crack tip. In fact, $(u_r - \Pi^h u_r)(x)$ vanishes on the nodes, thus

$$\|u_r - \Pi^h u_r\|_{L^\infty(K^*)} \leq \frac{C\alpha h_K^2}{\rho_K}, \tag{30}$$

then

$$\|u_r - \Pi^h u_r\|_{0,K^*} \leq \left[\int_{K^*}\left(C\alpha h_K^2\rho_K^{-1}\right)^2 dx\right]^{1/2} = C\alpha h_K^2\rho_K^{-1}\sqrt{meas(K^*)}, \tag{31}$$

and

$$|u_r - \Pi^h u_r|_{1,K^*} \leq \left[\int_{K^*}\left(C\alpha h_K\rho_K^{-1}\right)^2 dx\right]^{1/2} = C\alpha h_K\rho_K^{-1}\sqrt{meas(K^*)}. \tag{32}$$

Finally we can write the following estimates

$$\begin{aligned}\|u_r - \Pi^h u_r\|_{0,K^*} &\leq \left(Ch_K^3\rho_K^{-1}\right)\|u_r\|_{2+\epsilon,\Omega},\\ |u_r - \Pi^h u_r|_{1,K^*} &\leq \left(Ch_K^2\rho_K^{-1}\right)\|u_r\|_{2+\epsilon,\Omega}.\end{aligned} \tag{33}$$

Using (27) we obtain (26).

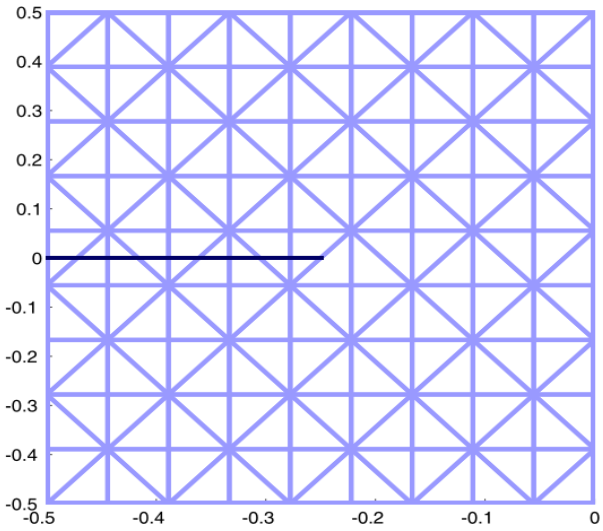

Figure 6. *Triangulation of* $\overline{\Omega}$.

Lemma 4.6. *Let* K *be a triangle partially enriched by* H *(fig.5 (b)), and* $K^* = K \setminus \Gamma_C$. *Over this triangle, the interpolation error can be bounded as follows*

$$\|u - \Pi^h u\|_{1,K^*} \;\leq\; Ch_K \sigma_K \|u - \chi u_s\|_{2+\epsilon,\Omega}. \tag{34}$$

Proof. We will estimate $\|u_r - \Pi^h u_r\|_{1,K^*}$ when K is the triangle partially enriched showed in fig.5 (b). The same work can be done for every other triangle partially enriched. In fact, $\Pi^h u_r$ over K^* can be written

$$\Pi^h u_r = \sum_{i=1}^{2} u_i(x_i)\varphi_i + \frac{u_1(x_3) + \widetilde{u_2}(x_3)}{2}\varphi_3 + \frac{u_1(x_3) - \widetilde{u_2}(x_3)}{2} H\varphi_3, \tag{35}$$

thus

$$\Pi^h u_r = \sum_{i=1}^{3} u_r(x_i)\varphi_i + \frac{\widetilde{u_2}(x_3) - u_1(x_3)}{2}\varphi_3 + \frac{u_1(x_3) - \widetilde{u_2}(x_3)}{2} H\varphi_3. \tag{36}$$

Using the imbedding result and the continuity of the extension operator, we can say that

$$\frac{u_1(x_3) - \widetilde{u_2}(x_3)}{2} \leq Cd\alpha, \tag{37}$$

$d \leq 2h$ denotes the maximal distance between a node of K and the crack tip, thus,

$$\|\nabla \Pi^h u_r\|_{\infty,K} \leq \frac{C\alpha d}{\rho_K}. \tag{38}$$

By repeating the same arguments of the proof of Lemma 4.5, we obtain the following

$$\begin{aligned} \|u_r - \Pi^h u_r\|_{0,K^*} &\leq \left(Ch_K^3 \rho_K^{-1}\right) \|u_r\|_{2+\epsilon,\Omega}, \\ |u_r - \Pi^h u_r|_{1,K^*} &\leq \left(Ch_K^2 \rho_K^{-1}\right) \|u_r\|_{2+\epsilon,\Omega}. \end{aligned} \tag{39}$$

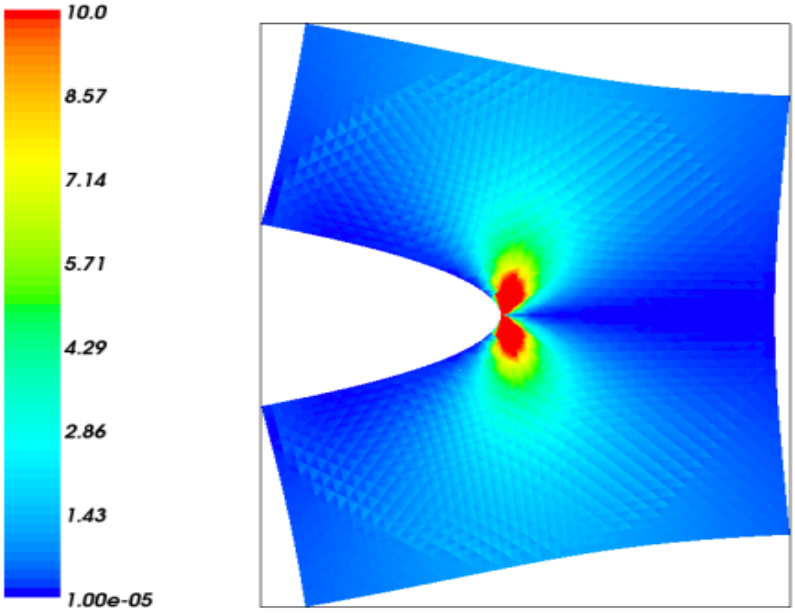

Figure 7. *Von Mises stress for the opening mode using a cut-off function.*

Finally, using (3), we can conclude the lemma's result. □

Proof of theorem 4.1. Using Cea's lemma, it is known that there exists $C_0 \geq 0$ such that

$$\|u - u^h\|_{1,\Omega} \leq C_0 \|u - v^h\|_{1,\Omega} \quad \forall v^h \in \vartheta^h, \tag{40}$$

thus

$$\|u - u^h\|_{1,\Omega} \leq C_0 \|u - \Pi^h u\|_{1,\Omega} \tag{41}$$

since $\Pi^h u \in \vartheta^h$. Using the local interpolation errors, the global error can be written

$$\|u - \Pi^h u\|^2_{1,\Omega} = \sum_{K^* \in \mathcal{T}_h} \|u - \Pi^h u\|^2_{1,K^*}. \tag{42}$$

where $K^* = K \setminus \Gamma_C$. The local interpolation error over the non-enriched triangles can obviously be derived from the global classical interpolation theorem, since we make a classical interpolation over these triangles. Then, for every non-enriched triangle K we have

$$\|u - \Pi^h u\|_{1,K} \leq C h_K \sigma_K \|u - \chi u_s\|_{2,K}. \tag{43}$$

Finally, the result of theorem 4.1 can be obtained using (43) and the lemmas 4.4, 4.5 and 4.6. □

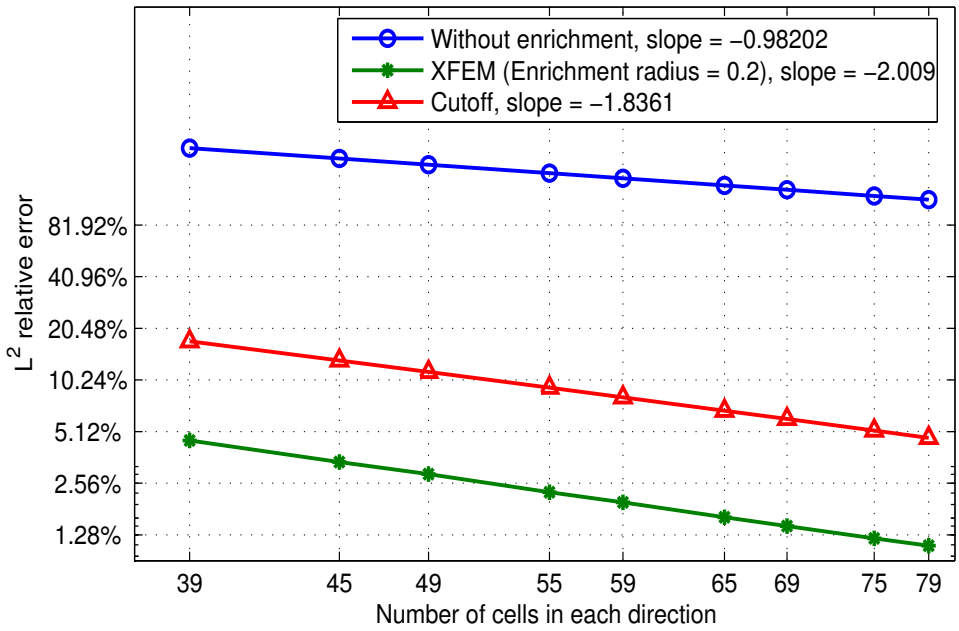

Figure 8. L^2 *error with respect to the number of cells in each direction (ns) for enriched P1 elements using a logarithmic scale.*

5. Numerical results

The non-cracked domain studied here is defined by $\overline{\Omega} = [-0.5; 0.5] \times [-0.5; 0.5]$ and the crack is the line segment $\Gamma_C = [-0.5; 0] \times \{0\}$. The opening mode displacement field is the exact solution prescribed as a Dirichlet condition on the domain boundary. The cut-off function $\chi \in C^2(\Omega)$ is defined such that

$$\begin{cases} \chi(r) = 1 \text{ if } r < r_0 = 0.01, \\ \chi(r) = 0 \text{ if } r > r_1 = 0.49, \end{cases} \tag{44}$$

and χ is identical to a fifth degree polynomial if $r_0 \leq r \leq r_1$. Note that by decreasing the difference between r_0 and r_1, the stiffness of χ increases and then the interpolation error is higher because of the presence of $\|u - \chi u_s\|_{2+\epsilon,\Omega}$ in the estimate of Theorem 4.1. Finally, the finite element method is the one defined in section 3 over a structured triangulation of $\overline{\Omega}$ (see Figure 6 for an example of a structured mesh of $\overline{\Omega}$). Note that the numerical tests are achieved using GETFEM++, an object oriented C++ finite element library (see [34]).

Figure 7 shows the von Mises stress over the opening mode deformed mesh of the model problem. As expected, the von Mises stress is concentrated at the crack tip (at the singularity). Figures 8 and 9 show a comparison between the convergence rates of the classical finite element method without enrichment, the XFEM method with a fixed enrichment area independent of

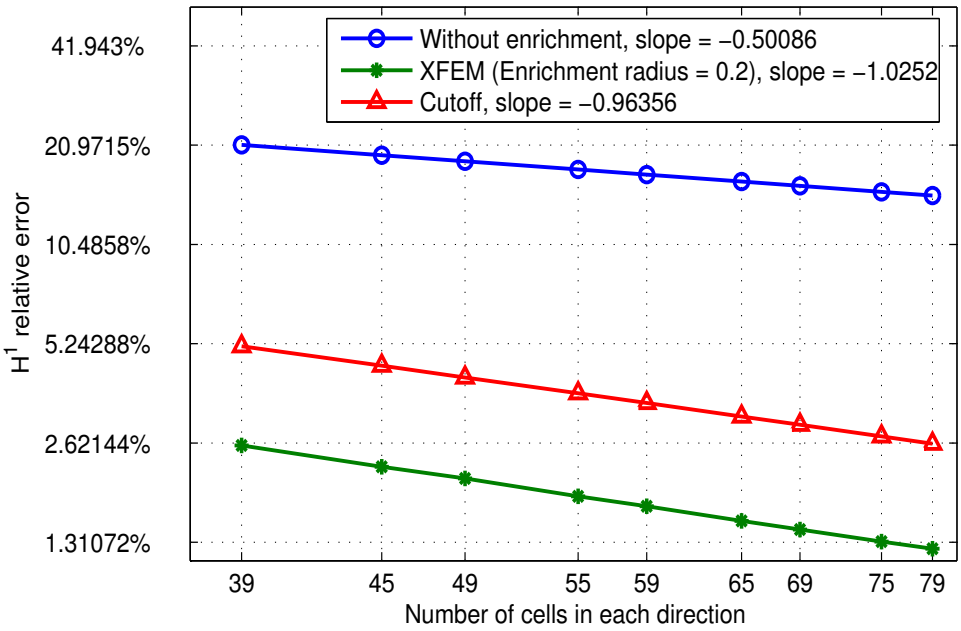

Figure 9. H^1 *error with respect to the number of cells in each direction (ns) for enriched P1 elements using a logarithmic scale.*

the parameter h and the cut-off enrichment strategy for the L^2 and the H^1 norms. These errors are obtained by running the test problem for some values of the parameter ns, where ns is the number of subdivisions (number of cells) in each direction ($h = 1/ns$). The rate of convergence for the L^2-norm is better than the one for the H^1-norm which is quite usual. However, The Aubin-Nitsche lemma cannot be directly applied here due to the weak regularity of the solution. Figure 9 confirms that the convergence rate for the energy norm is of order $\sqrt{h}$ for the classical finite element method without enrichment and of order h for the XFEM method over a fixed area. It shows also the optimal convergence obtained with the cut-off enrichment strategy.

The cut-off enrichment strategy improves the convergence rate of the method without enrichment and reduces the committed errors without a significant additional computational cost. This latter result represents an improvement of the classical XFEM method where the convergence rate remains of order $\sqrt{h}$ for many reasons detailed in [23]. Compared to the XFEM method with a fixed enrichment area (see [23] for more details), the convergence rate is very close but the error values are larger. The reason seems to be the influence of the "stiff" part of the cutoff function χ in the sense that its $H^2(\Omega)$-norm influences the error estimate bound given by Theorem 4.1. On the other hand, the cutoff enrichment reduces significantly the computational cost of XFEM with a fixed enrichment area where every degree of freedom over

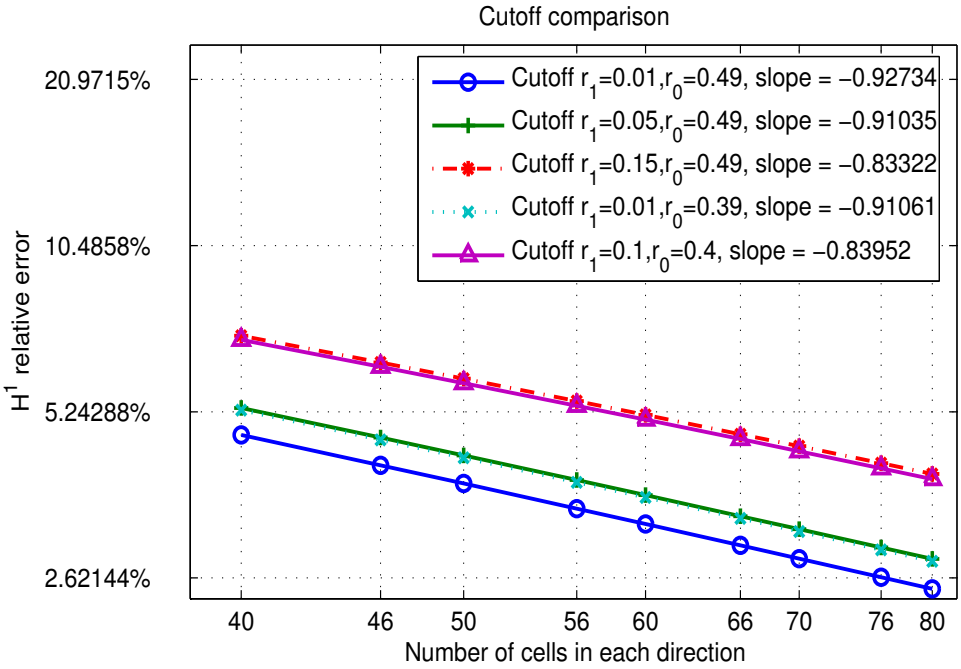

Figure 10. *Cutoff comparison using a logarithmic scale.*

this area is enriched by the singular displacement. This latter enrichment leads to a significant increase of the number of degrees of freedom method, but it eliminates the inconvenient of the classical XFEM where the support of the crack tip enrichment functions vanishes when h goes to 0. Table 5 shows a comparison between the number of the degrees of freedom for different refinements of the classical method, the XFEM with a fixed enrichment area and the cutoff method.

Table I. Number of degrees of freedom

Number of cells in each direction	Classical FEM	XFEM (enrichment radius =0.2)	Cutoff enrichment
40	3402	4962	3410
60	7502	11014	7510
80	13202	19578	13210

In order to test the influence of the cut-off enrichment radius, Figure 10 shows a comparison between different situations. The convergence rate is slightly modified. Although, the error level is better when the cut-off function is smoother. In other words the error level is influenced by the transition layer of the enrichment. This is again due to the influence of the $H^2(\Omega)$-norm

of the cutoff function (see (4.1)).

Figure 11 shows the variation of the von Mises stress over the vertical line of abscises 0.6 for the P_1 method presented above and also for a P_2 XFEM method still using a cut-off function. In the same time, as we can see in Figure 12, the conditioning of the linear system associated to the cut-off enrichment is very much better than the one associated to the XFEM with a fixed enrichment area. This is in particular due to the non-unisolvence of the XFEM classical enrichment (see [23]).

In order to explore the capabilities of the proposed variant, we consider a more sophisticated problem. In the following test, the exact solution is a combination of a regular solution to the elasticity problem, the mode I and the mode II analytical solutions and a higher order mode (for the deformed configuration, see Figure 13). The von Mises stress for this test is presented in Figure 13. Figure 14 shows a comparisons of the convergence curves of the non-enriched classical method, the XFEM and the cutoff strategy. The optimal rate is preserved for the cutoff enrichment.

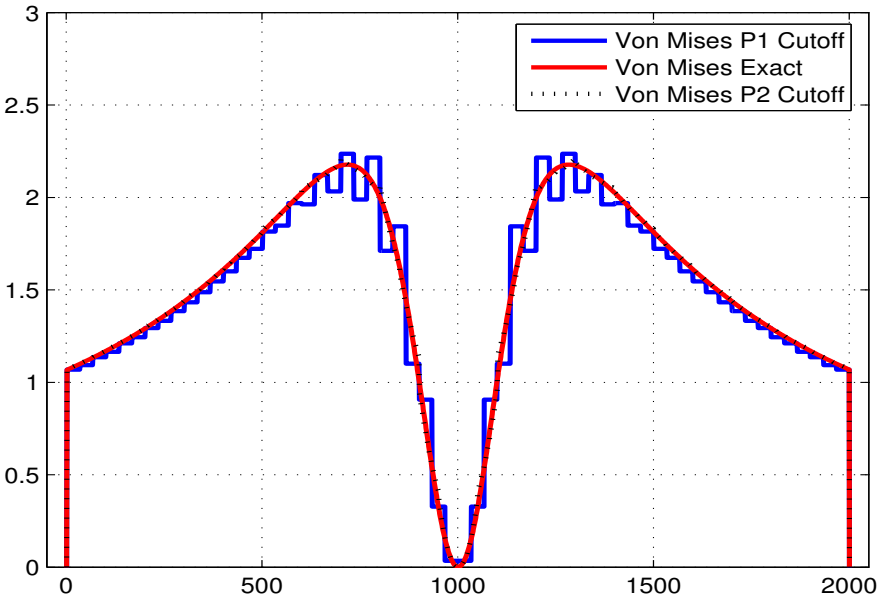

Figure 11. *Von Mises on the vertical* 0.6.

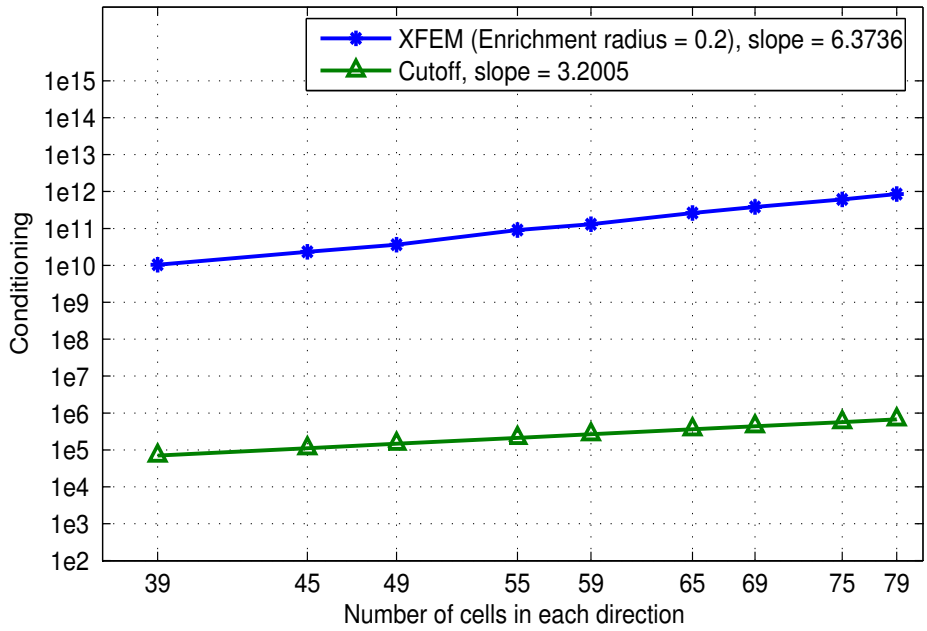

Figure 12. *Condition number of the linear system with respect to the number of cells in each direction (ns) using a logarithmic scale.*

Concluding remarks

The originality of this study consists mainly in the mathematical analysis of the transition between the crack tip singular enrichment and the discontinuous Heaviside enrichment. Concerning the XFEM with a fixed enrichment area, the mathematical analysis remains an open problem. However, the result presented here reinforces the confidence on the reliability of the XFEM methods. The presented cutoff strategy is limited to the 2D case. An adaptation to 3D problem is not straightforward and would require the use of a system of coordinates along the crack front. However, it is an appropriate method for 2D problems like cracked plate problems.

Acknowledgments

The authors would like to thank the anonymous referees for their helpful suggestions which permitted to improve the clarity and the legibility of the paper. Many thanks also to Julien Pommier for his support obtaining the numerical results.

REFERENCES

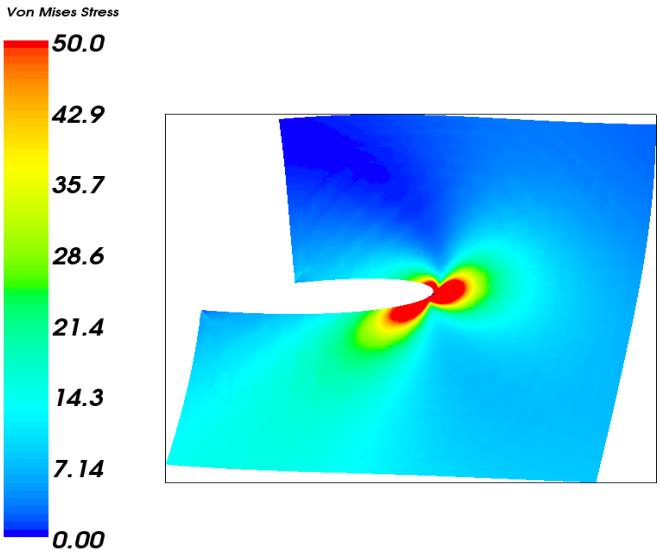

Figure 13. *Von Mises stress for a mixed mode using a cut-off function with P_2 elements.*

1. G. Strang, G. Fix. *An Analysis of the Finite Element Method.* Prentice-Hall, Englewood Cliffs, 1973.
2. J.M. Melenk and I. Babuška. The partition of unity finite element method: Basic theory and applications. *Comput. Meths. Appl. Mech. Engrg.*, 139:289–314, 1996.
3. H. Ben Dhia. Multiscale mechanical problems: the Arlequin method. *C. R. Math. Acad. Sci., Paris*, 326:899-904, 1998.
4. T. Strouboulis, I. Babuska, K. Copps. The design and analysis of the Generalized Finite Element Method. *Comput. Meths. Appl. Mech. Engrg.*, 181:43–69, 2000.
5. T. Strouboulis, I. Babuska, K. Copps. The generalized finite element method: an example of its implementation and illustration of its performance. *Int. J. Numer. Meth. Engng.*, 47:1401–1417, 2000.
6. N. Moës, J. Dolbow, and T. Belytschko. A finite element method for crack growth without remeshing. *Int. J. Numer. Meth. Engng.*, 46:131–150, 1999.
7. N. Moës, T. Belytschko. X-FEM: Nouvelles Frontières Pour les Eléments Finis. *Revue européenne des éléments finis (Calcul des structures GIENS'01), 11:305-318, 01/2002.*
8. N. Sukumar, N. Moës, B. Moran and T. Belytschko. Extended finite element method for three dimensional crack modelling. *Int. J. Numer. Meth. Engng.*, 48:1549–1570, 2000.
9. N. Moës, A. Gravouil and T. Belytschko. Non-planar 3D crack growth by the extended finite element and level sets, Part I: Mechanical model. *Int. J. Numer. Meth. Engng.*, 53(11):2549–2568, 2002.
10. A. Gravouil, N. Moës and T. Belytschko. Non-planar 3D crack growth by the extended finite element and level sets, Part II: Level set update. *Int. J. Numer. Meth. Eng.*, 53 (11):2569–2586, 2002.
11. P. M. A. Areias and T. Belytschko. Analysis of three-dimensional crack initiation and propagation using the extended finite element method. *Int. J. Numer. Meth. Engng., 63:760–788, 2005.*
12. T.C. Gasser and G.A. Holzapfel. Modeling 3D crack propagation in unreinforced concrete using PUFEM. *Comput. Methods Appl. Mech. Engrg., 194:2859–2896, 2005.*
13. T.C. Gasser and G.A. Holzapfel. 3D crack propagation in unreinforced concrete: A two-step algorithm for tracking 3D crack paths. *Comput. Methods Appl. Mech. Engrg., 195: 5198–5219, 2006.*
14. E. Wyart, D. Coulon, M. Duflot, T. Pardoen, Jean-Francois Remacle and Frédéric Lani. A substructured

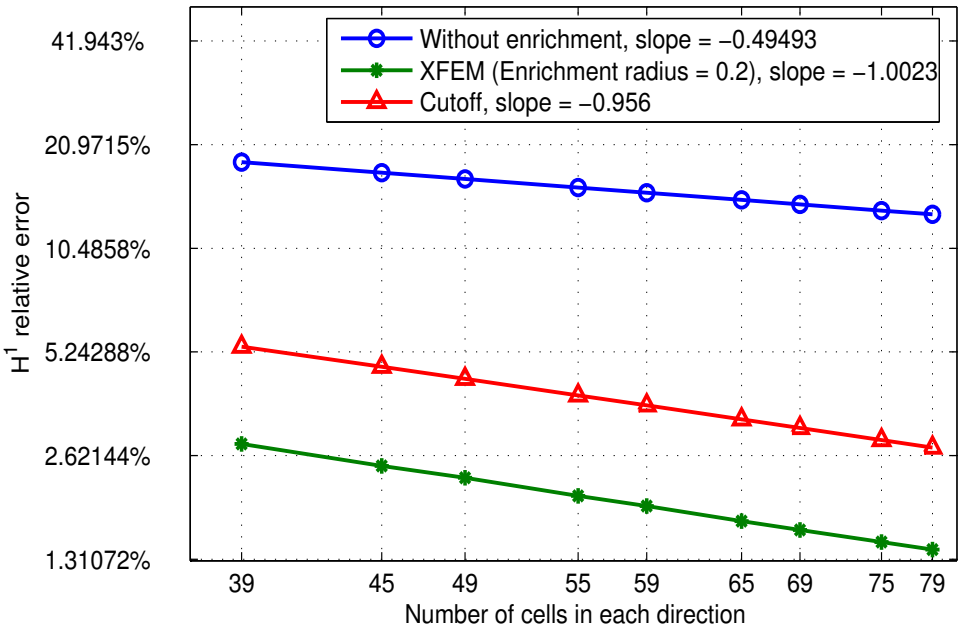

Figure 14. H^1 *error with respect to the number of cells in each direction (ns) for a mixed mode and enriched P1 elements using a logarithmic scale.*

FE-shell/XFE 3D method for crack analysis in thin walled structures. *Int. J. Numer. Meth. Engng., in press, 2007.*

15. S. Bordas, V.P. Nguyen, C. Dunant, H. Nguyen-Dang, and A. Guidoum. An extended finite element library. *Int. J. Numer. Meth. Engng., in press, 2007.*
16. E. Wyart, D. Coulon, P. Martiny, T. Pardoen, Jean-Francois Remacle and Frédéric Lani. A substructured FE/XFE method for stress-intensity factors computation in an industrial structure. *Revue Européenne de Mécanique Numérique, in press, 2007.*
17. E. Wyart, M. Duflot, D. Coulon, P. Martiny, T. Pardoen, J-F. Remacle and F. Lani. Substructuring FE-XFE approaches applied to three-dimensional crack propagation. *J. Comput. Appl. Math., in press, 2007.*
18. S. Bordas and B. Moran. Enriched Finite Elements and Level Sets for Damage Tolerance Assessment of Complex Structures. *Engng. Fract. Mech., 73:1176–1201, 2006.*
19. S. Bordas, J.G.C. Conley, B. Moran, J. Gray, and E. Nichols. A simulation-based design paradigm for complex cast components. *Engineering with Computers, 23 Issue 1:25–37, 2007.*
20. G. Ventura. On the elimination of quadrature subcells for discontinuous functions in the eXtended Finite-Element Method. *Int. J. Numer. Meth. Engng., 66:761–795, 2006.*
21. Q.Z. Xiao, B.L. Karihaloo. Improving the accuracy of XFEM crack tip fields using higher order quadrature and statically admissible stress recovery. *Int. J. Numer. Meth. Engng., 66:1378–1410, 2006.*
22. R. Glowinski, J. He, J. Rappaz, J. Wagner. Approximation of multi-scale elliptic problems using patches of elements. *C. R. Math. Acad. Sci., Paris*, 337:679–684, 2003.
23. P. Laborde, Y. Renard, J. Pommier, M. Salaun. High Order Extended Finite Element Method For Cracked Domains. *Int. J. Numer. Meth. Engng.* 64:354–381, 2005.
24. E. Béchet, H. Minnebo, N. Moës and B. Burgardt. Improved implementation and robustness study of the X-FEM for stress analysis around cracks. *Int. J. Numer. Meth. Engng.*, 64:1033–1056, 2005.
25. E. Chahine, P. Laborde, Y. Renard. A quasi-optimal convergence result for fracture mechanics with XFEM. *C. R. Math. Acad. Sci., Paris*, 342:527–532, 2006.

26. P. Grisvard. *Singularities in boundary value problems*. Masson, 1992.
27. P. Grisvard. Problèmes aux limites dans les polygones - Mode d'emploi. *EDF Bull. Directions Etudes Rech. Sér. C. Math. Inform. 1, MR 87g:35073, 21–59, 1986*.
28. J. Lemaitre, J.-L. Chaboche *Mechanics of Solid Materials*. Cambridge University Press, 1994.
29. J. B. Leblond. *Mécanique de la Rupture Fragile et Ductile*. Hermes, Lavoisier, 2003.
30. R. A. Adams. *Sobolev Spaces*. Academic Press, 1975.
31. P. G. Ciarlet. *The Finite Element Method For Elliptic Problems*. North Holland Publishing Company, 1979.
32. A. Hansbo, P. Hansbo. A Finite Element Method for the Simulation of Strong and Weak Discontinuities in Solid Mechanics. *Comput. Methods Appl. Mech. Engrg., 193:3523–3540, 2004*.
33. A. Ern, J.L. Guermond. *Eléments finis: théorie, applications, mise en œuvre*. Springer, 2001.
34. Y. Renard, J. Pommier. An open source generic C++ library for finite element methods. http://www-gmm.insa-toulouse.fr/getfem.